MEASURING GENERALIZED PARTON DISTRIBUTIONS

A. V. RADYUSHKIN

Physics Department, Old Dominion University, Norfolk, VA 23529,USA
and
Theory Group, Jefferson Lab, Newport News, VA 23606, USA

We discuss the basic theoretical aspects of hard exclusive electroproduction processes in quantum chromodynamics. They give access to generalized parton distributions, the hybrid functions having the features of the usual ("forward") parton densities, hadron distribution amplitudes and form factors. GPD's provide a unified description of several inclusive and exclusive processes, in particular, deeply virtual Compton scattering and hard electroproduction of ρ-mesons and pions, which can be investigated experimentally at Jefferson Lab.

I. HARD ELECTROPRODUCTION PROCESSES AND GENERALIZED PARTON DISTRIBUTIONS

The standard feature of applications of perturbative QCD to hard processes is the introduction of phenomenological functions accumulating information about nonperturbative long-distance dynamics. The well-known examples are the parton distribution functions $f_{a/H}(x)$ [1] used in perturbative QCD approaches to hard inclusive processes and distribution amplitudes $\varphi_\pi(x)$, $\varphi_N(x_1, x_2, x_3)$, which naturally emerge in the asymptotic QCD analyses of hard exclusive processes [2–7].

The parton distribution function $f_{a/H}(x)$ gives the probability that a fast-moving hadron H, with the momentum p contains a parton a carrying the momentum xp, and any other partons X (spectators) carrying together the remaining momentum $(1-x)p$. Schematically

$$f_{a/H}(x) \sim \sum_{\text{“}X\text{”}} |\Psi\{H(p) \to a(xp) + \text{“}X\text{”}\}|^2$$

where the summation is over all possible sets of spectators and $\psi\{H \to aX\}$ is the probability amplitude for the splitting process $H \to aX$.

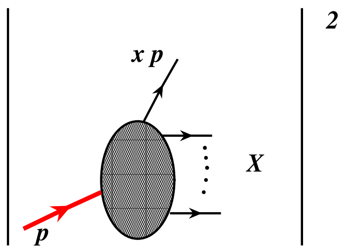

FIG. 1. Parton distribution function.

The summation over X reflects the *inclusive* nature of the description of the hadron structure by the parton distribution functions $f_{a/H}(x)$. On the other hand, the distribution amplitudes $\varphi(\{x\})$ correspond to *exclusive* description of the hadronic structure. For instance, $\varphi_{\pi^+}(x)$ gives the probability amplitude to find a (positive) fast-moving pion in a quark-antiquark state $u\bar{d}$, with the longitudinal pion momentum p shared in fractions x and $1-x$:

$$\varphi_{\pi^+}(x) \sim \Psi\{\pi^+(p) \to u(xp) + d((1-x)p)\} \ .$$

These two types of nonperturbative functions provide complementary information about the hadronic structure.

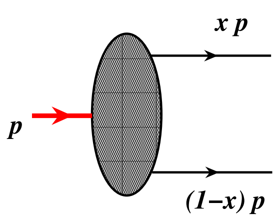

FIG. 2. Pion distribution amplitude.

The parton distribution functions $f_{a/H}(x)$ have been intensively studied in experiments on hard inclusive processes for the last 30 years. The classic process here is the deep inelastic scattering (DIS) $eN \to e'X$ whose structure functions are directly expressed in terms of parton distribution functions. The study of the perturbative QCD regime of hard exclusive reactions is a much more difficult task, due to small and rapidly decreasing cross sections. The high-luminosity electron accelerator facility of Jefferson Lab combined with high resolution and high acceptance spectrometers gives a unique opportunity to perform precision studies of hard exclusive electroproduction processes. On theoretical side, there was an essential development in the QCD description of these processes through the formalism which introduces new Generalized Parton Distributions (GPD's) ("Off-Forward" [8] and "Nonforward" [9] Parton Distributions are two implementations of GPD's). These distributions accumulating information about hadronic structure provide a unified description of wide variety of inclusive and exclusive hard processes.

In particular, the nonforward parton distribution $\mathcal{F}^a_\zeta(X,t)$ [9] gives the probability amplitude that the initial fast-moving hadron [having longitudinal momentum p] emits a parton a carrying the momentum Xp while the final-state hadron [having longitudinal momentum $p' = (1-\zeta)p$] absorbs a parton a carrying the momentum $(X-\zeta)p$:

$$\mathcal{F}^a_\zeta(X,t) \sim \sum_{\text{“}X\text{”}} \Psi\{H(p) \to a(xp) + \text{“}X\text{”}\} \times \Psi^*\{H((1-\zeta)p) \to a((X-\zeta)p) + \text{“}X\text{”}\}$$

where t is the invariant momentum transfer from the initial hadron to the final one.

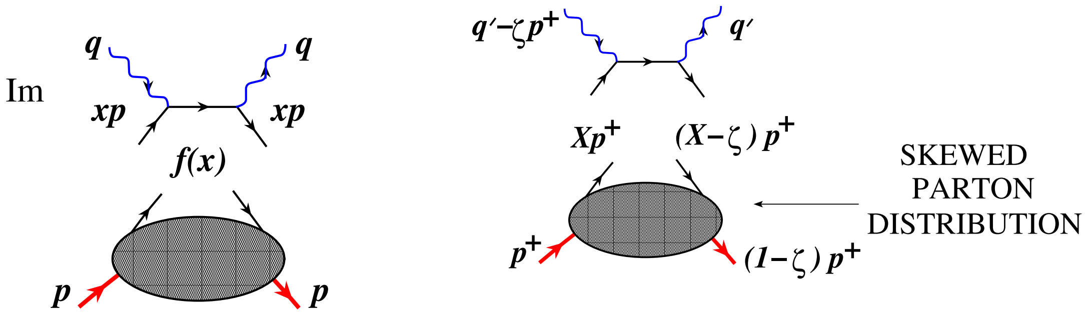

FIG. 3. Comparison of usual parton density $f(x)$ in DIS (left) and nonforward parton distribution $\mathcal{F}_\zeta(X,t)$ in DVCS (right).

The off-forward parton distributions $H^a(x,\xi;t)$ introduced by X. Ji [8] correspond to a description in which the initial and final hadron are treated in a symmetric way: the longitudinal momentum of the initial hadron is written as $(1+\xi)P$ and of the final one as $(1-\xi)P$. The longitudinal momentum of the initial parton is written as $(x+\xi)P$ and that of the final parton is written as $(x-\xi)P$. Here, $P = (p+p')/2$ is the average momentum of the initial and final hadron. Thus,

$$H^a(x,\xi;t) \sim \sum_X \Psi\{H(1+\xi) \to a(x+\xi) + \text{“}X\text{”}\} \times \Psi^*\{H(1-\xi) \to a(x-\xi) + \text{“}X\text{”}\} \ .$$

In the forward limit, when $p = p'$ [i.e., $t = 0$ and $\zeta = 0$ or $\xi = 0$], the Generalized Parton Distributions coincide with the usual parton densities measured in inclusive processes such as deep inelastic scattering. This a nontrivial prediction of quantum chromodynamics. Furthermore, in a nonforward kinematics, GPD's contain much richer information about the parton correlations. The latter can be nondiagonal in
(i) hadron/parton momenta,
(ii) hadron/parton spin, and even
(iii) can correspond to different hadrons in the initial and final state, e.g., one can consider matrix elements corresponding to $p \to n$, $N \to \Delta$, $N \to \Lambda$ etc. transitions.

Thus, GPD's provide detailed information about the nucleon structure: they are sensitive not not only to probabilities but also to interference between different components of the nucleon wave function.

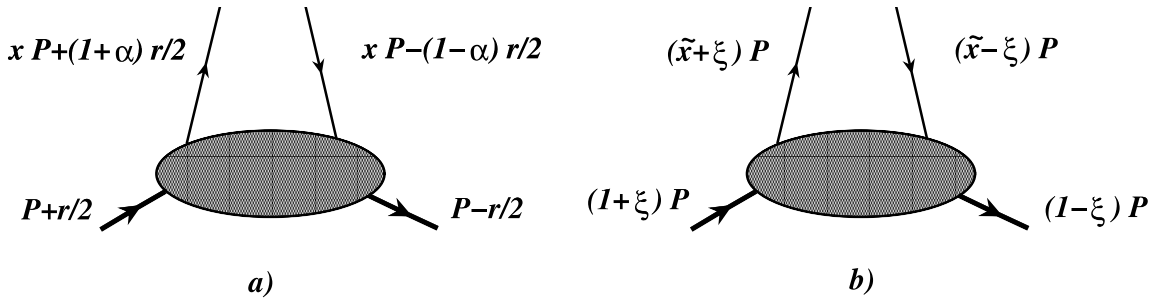

FIG. 4. Description of the nonforward matrix element in terms of a) symmetric double distribution $f(x, \alpha; t)$ and off-forward parton distribution $H(\tilde{x}, \xi; t)$.

GPD's depend on the invariant momentum transfer t, just like elastic form factors. Hence, GPD's may be also treated as generalizations of hadronic form factors to which they are related by "reduction" formulas

$$\int_0^1 \mathcal{F}_\zeta^a(X,t)\,dX = F^a(t) \ .$$

Just like form factors, GPD's include, in general, the functions which are non-diagonal in hadronic spin; compare with the nucleon spin-flip form factor $F_2(t)$ corresponding to the anomalous magnetic moment. The forward limit of the relevant GPD [$E(x,\xi;t)$ in Ji's notations] exists, but it cannot be accessed in inclusive measurements which are sensitive only to spin-diagonal parton distributions. The intriguing observation of Ji [8] is that the x-moment

$$J_q = \frac{1}{2}\int_{-1}^{1} \{H(x,\xi=0;t=0) + E(x,\xi=0;t=0)\}\, x\, dx$$

measures the total contribution [due to both the spin and orbital momentum] of the quarks to the nucleon spin. Ji proposed to use Deeply Virtual Compton Scattering (DVCS) to get access to the $E(x,\xi=0;t=0)$ function. This function can be also accessed in hard meson electroproduction processes. These findings triggered the recent interest to GPD's and hard meson and photon electroproduction processes. From further studies of these processes it became clear that they are very interesting on their own grounds.

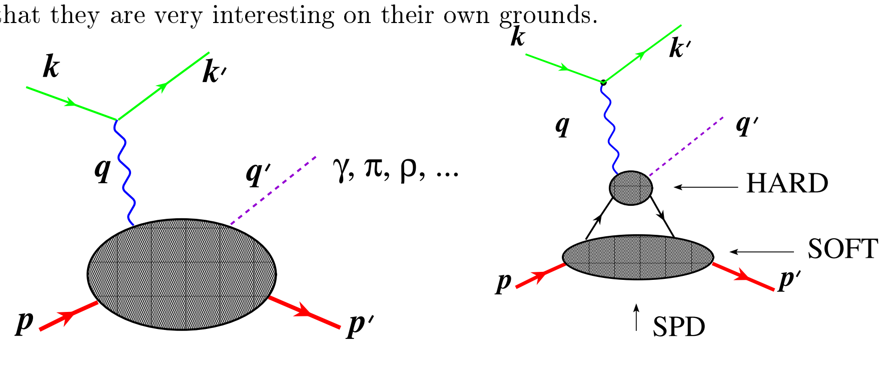

FIG. 5. Hard electroproduction processes. Left: general structure; right: perturbative QCD factorization.

In particular, the physics of hard electroproduction processes includes the following features:

1. **Scaling.** DVCS and hard meson electroproduction processes depend on 3 momentum invariants: initial photon virtuality $q^2 = -Q^2$, initial photon energy in the lab frame ν: $(pq) = m\nu$, invariant momentum

transfer $t = (p - p')^2$. The nontrivial prediction of perturbative QCD is that for fixed t and sufficiently large Q^2 and (pq), the hard exclusive electroproduction amplitudes have a simple scaling structure $\Phi(x_{Bj})/Q^N$, with a calculable integer power N [it is determined by the dimensional analysis] and the function $\Phi(x_Bj)$ depending only on the Bjorken ratio $Q^2/2(pq) \equiv x_{Bj}$. This prediction reflects the basic pointlike nature of the quarks and the fundamental short-distance properties of quantum chromodynamics such as asymptotic freedom.

2. **Exclusive-inclusive connection.** As already emphasized, another nontrivial prediction of QCD is that the generalized parton distributions $H(x, \xi; t)$ describing the *amplitudes* of purely *exclusive* processes like DVCS process $\gamma^* N \to \gamma N$ are directly related to the usual parton densities $f(x)$ describing the *cross sections* of *inclusive* processes like DIS process $\gamma^* N \to X$.

3. **Electroproduction – form factor connection.** Since the integrals of GPD's are related to hadronic form factors, the t-dependences of hard electroproduction amplitudes and elastic form factors are interconnected.

II. SKEWEDNESS

The factorized amplitudes of deeply virtual Compton scattering (DVCS) and hard exclusive electroproduction processes [8–11] involve nonforward matrix elements $\langle p' | \ldots | p \rangle$. The crucial observation is that the kinematics of hard elastic electroproduction processes in which a highly virtual photon is converted into a massless photon or a low-mass meson requires the presence of the longitudinal component in the momentum transfer $r \equiv p - p'$ from the initial baryon to the final one: $r^+ = \zeta p^+$ (or $r^+ = 2\xi P^+$). This means that the nonperturbative matrix element $\langle p' | \ldots | p \rangle$ is essentially asymmetric (skewed) even for $t = 0$. For DVCS and meson electroproduction in the region $Q^2 \gg |t|, m_H^2$, the "skewedness" parameter ζ of nonforward parton distributions $\mathcal{F}_\zeta(X; t)$ coincides with the Bjorken variable

$$\zeta = x_{Bj} = Q^2/2(pq) \ .$$

The skewedness parameter ξ of the off-forward parton distributions $H(x, \xi; t)$ is related to x_{Bj} by

$$\xi = \frac{x_{Bj}}{2 - x_{Bj}} \ .$$

Note that both ζ and ξ vary between 0 and 1.

Generalized parton distributions parameterize nonforward matrix elements of nonlocal quark operators $\langle p' | \bar{\psi}(z_2) \Gamma \psi(z_1) | p \rangle$. Hence, they are a generalization of hadronic form factors. The latter correspond to local currents $\langle p' | \bar{\psi}(0) \Gamma \psi(0) | p \rangle$. GPD's are also related to the usual parton densities $f(x)$ measured in hard *inclusive* processes like deep inelastic scattering. In the latter case, one deals with the inclusive cross section related *via* optical theorem to the virtual forward Compton amplitude. This is a symmetric situation when the same momentum p appears in both brackets of the hadronic matrix element $\langle p | \bar{\psi}(z_2) \Gamma \psi(z_1) | p \rangle$, which corresponds to zero skewedness.

III. COMPTON AMPLITUDES AS A PROBE OF HADRONIC STRUCTURE

Diagrammatically, the "handbag" contribution to a general Compton amplitude is the simplest physical process in which one deals with parton distributions. Hence, to establish a connection between different types of parton distributions, it is instructive to consider the Compton amplitude in the most general case. From the physical point of view, the Compton scattering in its various versions provides a unique tool for studying many aspects of hadronic structure.

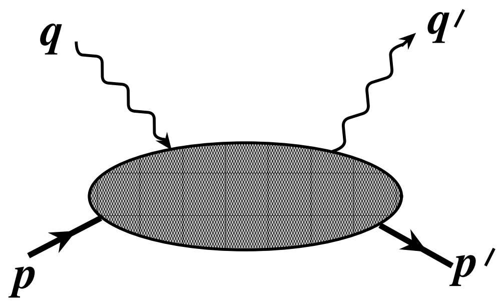

FIG. 6. General Compton amplitude.

A general Compton amplitude is a four-point function $T^{\mu\nu}(q,p,q',p';\sigma_1,\sigma_2)$ in which the hadronic structure is probed by two electromagnetic currents. In QCD, the photons couple to the quarks of the hadron. In the simplest approximation, the photon-quark vertex is pointlike. However, in the soft regime, strong interactions produce corrections uncalculable within the perturbative QCD framework. To preserve the simple pointlike structure of the photon-quark coupling, one should incorporate the asymptotic freedom property of quantum chromodynamics and choose a specific kinematics in which the behavior of the relevant amplitude is dominated by short distances. An essential feature of all such types of kinematics is the presence of a large momentum transfer.

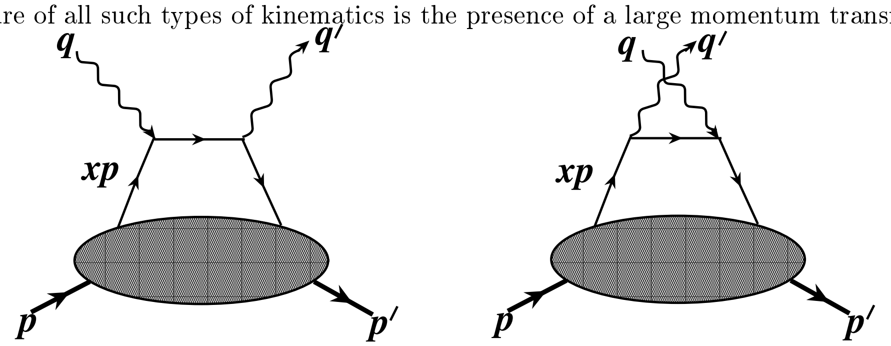

FIG. 7. Handbag contribution to the Compton amplitude.

Deep inelastic scattering. The short-distance dominance is secured by high virtuality of the photons: $-q'^2 = -q^2 \equiv Q^2 > 1$ GeV^2. The total cm energy of the photon-hadron system $s = (p+q)^2$ should be above resonance region, and the Bjorken ratio $x_{Bj} = Q^2/2(pq)$ is finite. DIS gives information about usual parton densities $f_a(x), \Delta f_a(x)$. The dominant leading-order contribution corresponds to the handbag diagram in which the parton amplitude is given by hard quark propagator proportional to $1/[(xp+q)^2 + i\epsilon]$. Its imaginary part contains the $\delta(-Q^2 + 2x(qp))$ factor (terms $O(p^2)$ are neglected) which selects just the $x = x_{Bj}$ value from the integral over the momentum fraction x. As a result, the DIS cross section is expressed in terms of $f(x_{Bj})$, $\Delta f(x_{Bj})$. More specifically, the Compton amplitude is

$$T(Q^2,(qp)) \sim \sum_a e_a^2 \int_{-1}^{1} f^a(x) \left[\frac{1}{x - x_{Bj} + i0} + \frac{1}{x + x_{Bj} - i0} \right] dx \ + \dots \ , \tag{3.1}$$

where the convention is that the $0 < x < 1$ part of $f^a(x)$ corresponds to the quark distribution and the $-1 < x < 0$ part to the (minus) antiquark distribution. The imaginary part, hence, is given by a sum of

$$e_q^2[f^q(x_{Bj}) + f^{\bar{q}}(x_{Bj})]$$

terms.

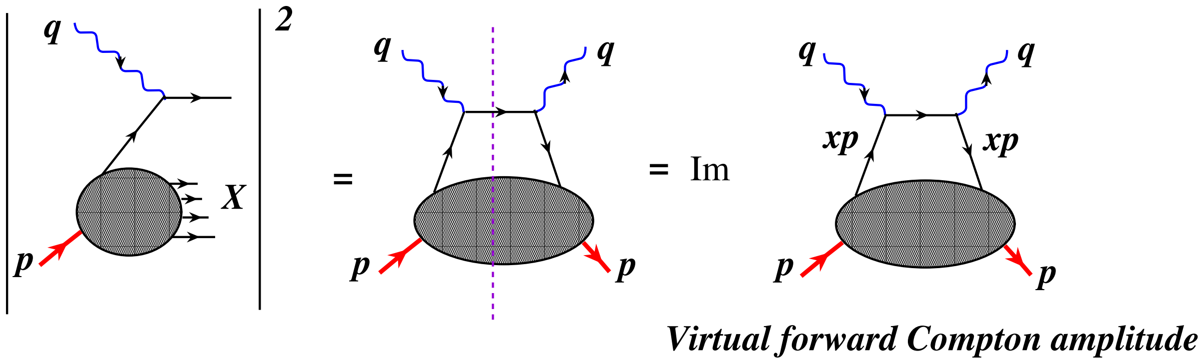

FIG. 8. Cross section of DIS as imaginary part of the virtual forward Compton amplitude.

Deeply virtual Compton scattering. In DVCS, the initial photon is highly virtual ($q^2 \equiv -Q^2$ is large) while the final photon is real: $q'^2 = 0$. To make the contact with the usual ("forward") parton densities, the momentum transfer t should be made as small as possible. Having large virtuality of the initial photon is sufficient for QCD factorization [9,12,13]. The relevant formula for DVCS has the structure similar to that valid in the forward case; e.g., the invariant amplitude symmetric in the photon μ, ν indeces looks like

$$T(Q^2, p\cdot q, t) \sim \sum_a e_a^2 \int_{-1}^{1} H^a(x,\xi;t) \left[\frac{1}{x-\xi+i0} + \frac{1}{x+\xi-i0} \right] dx \ + \dots \ . \tag{3.2}$$

In addition to the "usual" momentum fraction x, the generalized parton distribution $H^a(x,\xi;t)$ (to be specific, here and in the following, we use the OFPD notations of Ji [8]) also depends on the invariant momentum transfer $t = (p'-p)^2$ and the skewedness parameter $\xi = r^+/2P^+$ (where $r \equiv p - p'$, $P = (p+p')/2$) specifying the longitudinal momentum asymmetry of the nonforward matrix element.

For fixed t [and for each GPD], one deals with two functions $I(\xi,t)$ and $R(\xi,t)$ of the skewedness parameter ξ (or eventually, of the Bjorken variable x_{Bj}) corresponding to the real and imaginary parts of $T(Q^2, p\cdot q, t)$. The latter is proportional to $H^a(x=\xi,\xi;t)$ or to an extremely asymmetric situation when the initial parton carries the longitudinal momentum $2\xi P^+ = x_{Bj} p^+$ while the fraction $x' = x - \xi$ corresponding to the "final" parton vanishes. Existing models for GPD's [14,15] give rather specific predictions for $I(\xi,t)$ and $R(\xi,t)$, which should be compared with future experimental data.

IV. RELATION OF GPDS TO FORM FACTORS AND PARTON DENSITIES

In some limiting cases, generalized parton distributions reduce to simpler functions which have been already studied experimentally. For instance, if $p = p'$, i.e., $r = 0$, the matrix element coincides with the forward one which defines the usual parton distribution function. This results in

$$H_a(x, \xi = 0; t = 0) = f_a(x)\,;\ . \tag{4.1}$$

Integrating $H(x,\xi,t)$ over x one obtains hadronic form factors:

$$\sum_a e_a \int_{-1}^{1} H(x,\xi,t)\, dx = F_1(t)\,, \tag{4.2}$$

where e_a is the electric charge of the relevant quark. Just like for form factors, there are extra generalized parton distributions $E(x,\xi,t)$ corresponding to helicity flip in the nonforward matrix element. They are related to $F_2(t)$ form factor:

$$\sum_a e_a \int_{-1}^{1} E(x,\xi,t)\,dx = F_2(t)\,. \tag{4.3}$$

Note that though the shape of GPD's changes when ξ is varied, the integrals (4.2),(4.3) do not depend on ξ. Since the E functions are accompanied by the r_μ factor in the parameterization of the nonforward matrix element

$$\langle p'|\bar{\psi}\gamma_\mu\psi|p\rangle \sim \bar{u}(p')\gamma_\mu u(p)\text{“}H\text{”} + \frac{1}{2M}\bar{u}(p')\sigma_{\mu\nu}r^\nu u(p)\text{“}E\text{”}\ ,$$

they are invisible in deep inelastic scattering described by exactly forward $r=0$ Compton amplitude. However, the $t=0, \xi=0$ limit of the E distributions exists:

$$E_a(x,\xi=0;t=0) \equiv e_a(x)\ .$$

In particular, for $t=0$ the integral (4.3) gives the anomalous magnetic moment. Moreover, the renewed interest to DVCS and generalized parton distributions is due to observation made by X. Ji [8] that the integral

$$J_q = \frac{1}{2}\sum_a \int_{-1}^{1} [f_a(x)+e_a(x)]\ xdx \tag{4.4}$$

is related to the total spin and orbital momentum contribution of the quarks into the proton spin.

The DVCS amplitude contains two other generalized parton distributions $\tilde{H}(x,\xi;t)$ and $\tilde{E}(x,\xi;t)$. The $\tilde{H}$-distributions reduce in the forward limit to the polarized parton distributions $\tilde{H}(x,\xi=0;t=0) = \Delta f^a(X)$ and contribute to the axial form factor $G_A(t)$ after the x-integration. Similarly, the functions $\tilde{E}(x,\xi;t)$ are related to the pseudoscalar form factor. At small t, they are dominated by the pion pole term $1/(t-m_\pi^2)$.

V. MODELING GPDS

There are two approches used to model GPDs. One is based on direct calculation of parton distributions in specific dynamical models, such as bag model [19], chiral soliton model [20], light-cone formalism [21], etc. Another approach [16,22,14] is a phenomenological construction based on reduction formulas relating GPDs to usual parton densities $f(x), \Delta f(x)$ and form factors $F_1(t), F_2(t), G_A(t), G_P(t)$. The most convenient way to construct such models is to start with “double distributions” $f(\tilde{x},\alpha;t)$ [23]. The use of double distributions is an alternative way to parameterize a nonforward matrix element.

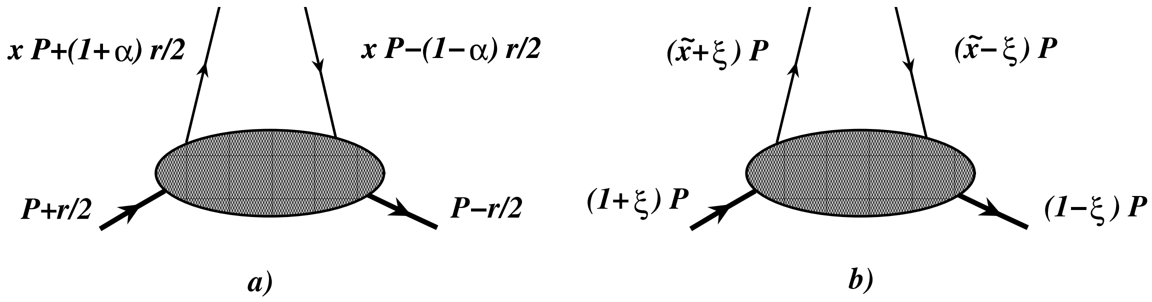

FIG. 9. Description of the nonforward matrix element in terms of a) symmetric double distribution $f(x,\alpha;t)$ and off-forward parton distribution $H(\tilde{x},\xi;t)$.

In the DD picture the parton momentum $k^+ = \tilde{x}P^+ + (1+\alpha)r^+/2$ comes both from the average momentum P^+ and the momentum transfer r^+. Though the "plus" components of r and P are proportional to each other $r^+ = 2\xi P^+$, one should make a clear distinction between them, since they specify the momentum flow in two different channels. For $r = 0$, the momentum flows only in the s-channel. In this case, the matrix element coincides with the usual (forward) distribution function. The outgoing parton cariies the same momentum xP as the incoming one. On the other hand, if $P = 0$, but $r \neq 0$, the matrix element has the structure of the distribution amplitude in which the momentum r^+ splits into the fractions $(1+\alpha)r^+/2$ and $(1-\alpha)r^+/2$ carried by the quarks. In a combined situation, when both P and r are nonzero, the initial quark has the momentum $\tilde{x}P^+ + (1+\alpha)r^+/2$, while the final one carries the momentum $\tilde{x}P^+ - (1-\alpha)r^+/2$. This suggests that the $\tilde{x}$-profile of DDs $f(\tilde{x},\alpha)$ is driven by the shape of the usual parton density $f(\tilde{x})$ while their α profiles are analogous to the shape of two-body distribution amplitudes like $[(1-\tilde{x})^2-\alpha^2]^n$ (the support properties of DDs [23] require $|\alpha| \leq 1-|x|$). Fixing the profile width parameter n gives simple models [16] for DDs which can be converted into models for GPD's after the appropriate integration

$$H(x,\xi) = \int_{-1}^{1} d\tilde{x} \int_{-1+|\tilde{x}|}^{1-|\tilde{x}|} \delta(\tilde{x}+\xi\alpha - x)\, f_i(\tilde{x},\alpha)\, d\alpha \ . \tag{5.1}$$

The δ-function here reflects the fact that

$$k^+ = \tilde{x}P^+ + \frac{1}{2}(1+\alpha)r^+ = [\tilde{x} + (1+\alpha)\xi]P^+ = (x+\xi)P^+ \ .$$

Due to the hermiticity properties and time-reversal invariance, the DD's $f(\tilde{x},\alpha)$ should be even functions of α ("Munich symmetry" [22]). Thus, for the limiting case $t = 0$ one can try a factorized ansatz $f(\tilde{x},\alpha) = h(\tilde{x},\alpha)\, f(\tilde{x})$, where $h(\tilde{x},\alpha)$ is a profile function even in α. It is fixed by the relation connecting $f(\tilde{x},\alpha)$ with forward densities

$$\int_{-1+|x|}^{1-|x|} f(x,\alpha)\, d\alpha = f(x)\,. \tag{5.2}$$

For example, the $n = 1$ profile function is $h^{(1)}(\tilde{x},\alpha) = \frac{3}{4}[(1-\tilde{x})^2 - \alpha^2]/(1-|\tilde{x}|)^3$. A simple parameterization $f(x) = (1-|x|)^3/x$ for singlet quark distributions gives an explicit model for quark GPDs. Resulting curves for the family of $H(x,\xi)$ functions are shown in Fig.10.

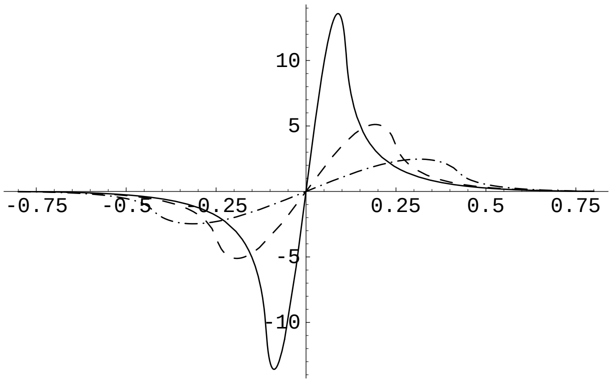

FIG. 10. Singlet quark distribution $H_S^1(\tilde{x},\xi)$ for several ξ values 0.1 (full), 0.25 (dashed), 0.4 (dot-dashed). Forward distribution is modeled by $(1-x)^3/x$.

In a similar way, one can construct ansätze for nonsinglet distributions and for functions $f(\tilde{x},\alpha;t)$ involving nonzero t values. For the infinitely narrow profile function $f^{(\infty)}(\tilde{x},\alpha) = \delta(\alpha)f(\tilde{x})$, the relation between GPD's and usual densities is especially simple: $H(x,\xi) = f(x)$. Hence, the practically interesting function $H(x=\xi,\xi)$ (determining the magnitude of the imaginary part of the DVCS amplitude) in this case is $f(\xi)$, or in terms of the

Bjorken variable $f(x_{Bj}/(2-x_{Bj}))$; i.e., the imaginary part of $t=0$ DVCS amplitude can be approximated by usual forward densities with the argument which for small $f(x_{Bj})$ is approximately twice smaller than in deep inelastic scattering. This results in the "GPD enhancement factor" [16]: if $f(x) \sim x^{-a}$ for small x, the ratio $H(\xi,\xi)/f(x_{Bj})$ is 2^a. The effect is sizable, e.g., for $f(x) \sim 1/\sqrt{x}$ the enhancement factor is $\sqrt{2}$ for the amplitude and 2 for the cross section, which is a good news from the experimental point of view. For a wider profile function the enhancement factor is larger, e.g., for the $h^{(1)}(\tilde{x},\alpha)$ model, the enhancement factor is $1/[(1-x_{Bj})^2(1-a/2)(1-a/3)]$ which gives $8/5$ for $a=0.5$ and small x_{Bj}. The enhancement strongly increases when x_{Bj} is not small.

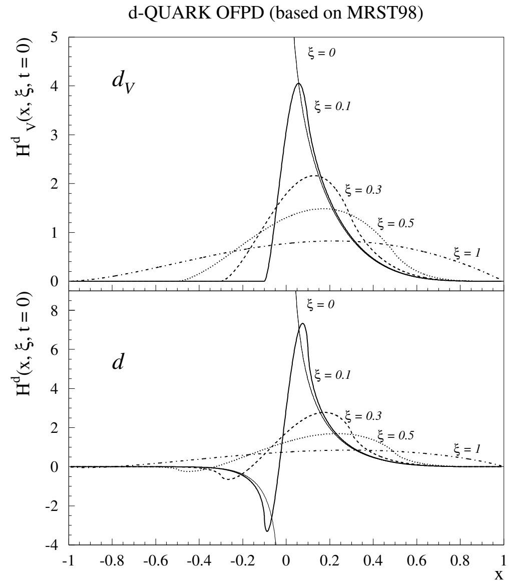

FIG. 11. Quark distributions $H^1_d(\tilde{x},\xi)$ for several ξ values, with the forward d-quark distributions taken from the MRST parameterization [27]

VI. DEEPLY VIRTUAL COMPTON SCATTERING

An important practical question is at which Q^2 are large enough to ensure the dominance of the lowest-twist handbag contribution. To get an estimate for the onset of the scaling phenomena, we can compare DVCS to similar processes. In DIS, approximate Bjorken scaling starts at $Q^2 \sim 2\,\mathrm{GeV}^2$. It is even more appropriate to look at experimental data for the exclusive process $\gamma(q_1)\gamma^*(q_2) \to \pi^0$ studied on e^+e^- colliders. If one of the photons is highly virtual $q_1^2 = -Q^2$ while another is (almost) real $q_2^2 \sim 0$, the process is kinematically similar to DVCS. In the leading order of QCD, the $F_{\gamma\gamma^*\pi^0}(Q^2)$ transition form factor is given by a handbag diagram. The recent measurements by CLEO [26] show that the pQCD prediction $F_{\gamma\gamma^*\pi^0}(Q^2) \sim 1/Q^2$ again works starting from $Q^2 \sim 2\,\mathrm{GeV}^2$ (see Fig. 12).

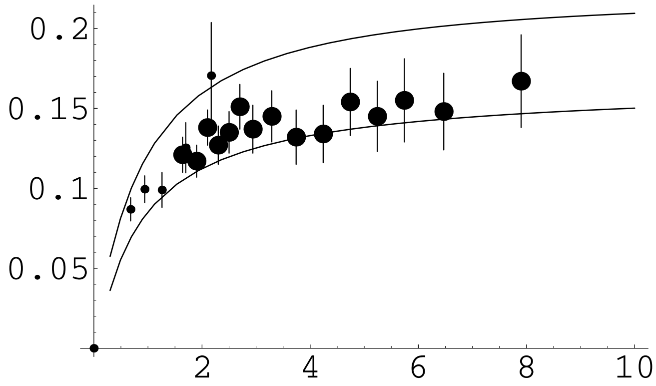

FIG. 12. Comparison of experimental data on $\gamma^*\gamma\pi^0$ form factor with next-to-leading order pQCD predictions using asymptotic shape for the pion distribution amplitude (lower curve) and Chernyak-Zhitnitsky model (upper curve).

The $\gamma\gamma^*\pi^0$ vertex (for a virtual pion) can be also measured on a fixed-target machine in which case it is just a part of the DVCS amplitude corresponding to the $\tilde{E}(x,\xi;t)$ generalized parton distribution. Hence, CLEO data give an evidence that DVCS may be handbag-dominated for Q^2 as low as $2\,\mathrm{GeV}^2$.

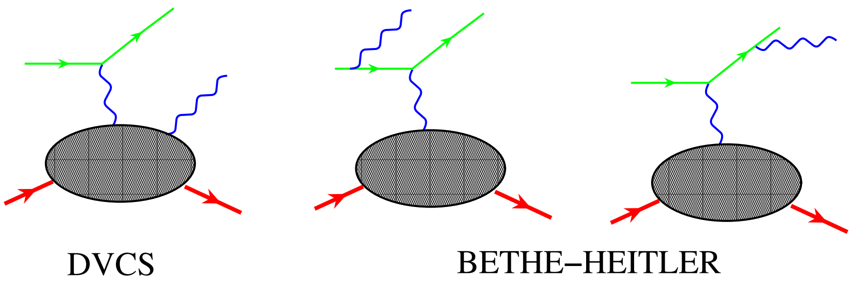

FIG. 13. DVCS and Bethe-Heitler contribution to the $eN \to e'N'\gamma$ process.

The main complication for studying DVCS is the contamination by the Bethe-Heitler process in which the final photon is emitted from the initial or final electron. The Bethe-Heitler amplitude is enhanced at small t

$$\mathcal{A}^{DVCS} \sim \frac{1}{Q^2} T^{DVCS} \quad ; \quad \mathcal{A}^{BH} \sim \frac{1}{t}\frac{1}{(k-q')^2 - m_e^2} + \frac{1}{t}\frac{1}{(k'+q')^2 - m_e^2} \ . \tag{6.1}$$

Since the virtual photon flux for fixed Q^2 and x_{Bj} increases when the electron beam energy increases, the upgrade of the JLab accelerator to 12 GeV has many advantages for the studies of DVCS.

Furthermore, the interference between the Bethe-Heitler process and DVCS can be used for the amplification of the DVCS signal. The crucial fact is that DVCS amplitude $\mathcal{A}^{DVCS}$ has both real and imaginary parts while $\mathcal{A}^{BH}$

is purely real, and one can incorporate the interference between DVCS and Bethe-Heitler amplitudes to disintangle Re $\mathcal{A}^{DVCS}$ and Im $\mathcal{A}^{DVCS}$.

In particular, measuring the single-spin asymmetry gives access to the imaginary part of the DVCS amplitude

$$\frac{d^5 \overrightarrow{\sigma} - d^5 \overleftarrow{\sigma}}{d^5 \overrightarrow{\sigma} + d^5 \overleftarrow{\sigma}} \sim \mathrm{Im}\,(T^{DVCS} T^{BH}) \sim \mathrm{Im}\, T^{DVCS} \ . \tag{6.2}$$

This asymmetry vanishes in the collinear kinematics. Hence, to calculate it reliably one should keep in the DVCS amplitude the terms proportional to the transverse component r_T of the momentum transfer $r = p - p'$. These terms are also necessary to guarantee gauge invariance of the DVCS amplitude with respect to electromagnetic interaction. The approach allowing to include such non-leading twist-3 terms was developed in a recent paper [31].

Another asymmetry is due to the beam charge change, and it is proportional to the real part of the DVCS amplitude

$$\frac{d^5\sigma^- - d^5\sigma^+}{d^5\sigma^- + d^5\sigma^+} \sim \mathrm{Re}\,(T^{DVCS} T^{BH}) \sim \mathrm{Re}\, T^{DVCS} \ . \tag{6.3}$$

To measure this asymmetry, one needs a positron beam. Note that in both cases the asymmetry is linear in the DVCS amplitude.

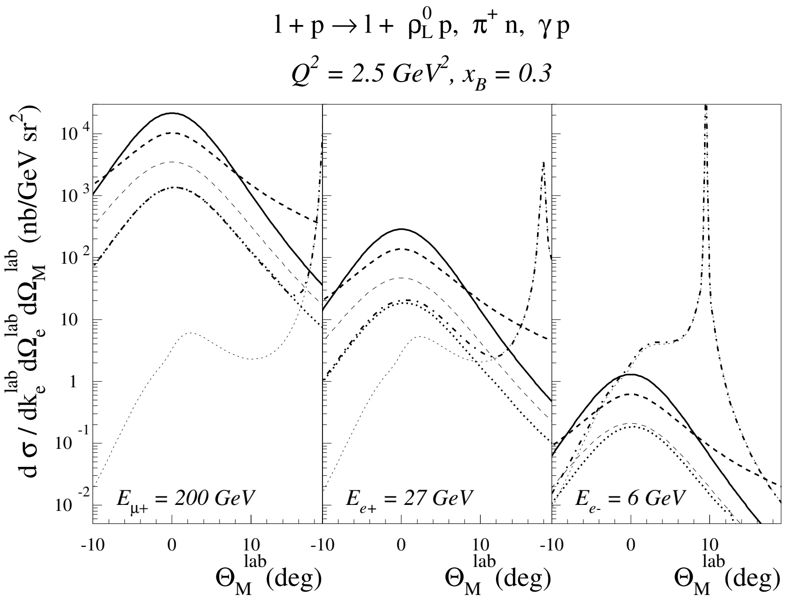

FIG. 14. Comparison of cross sections for hard electroproduction of photons and mesons for different energies.

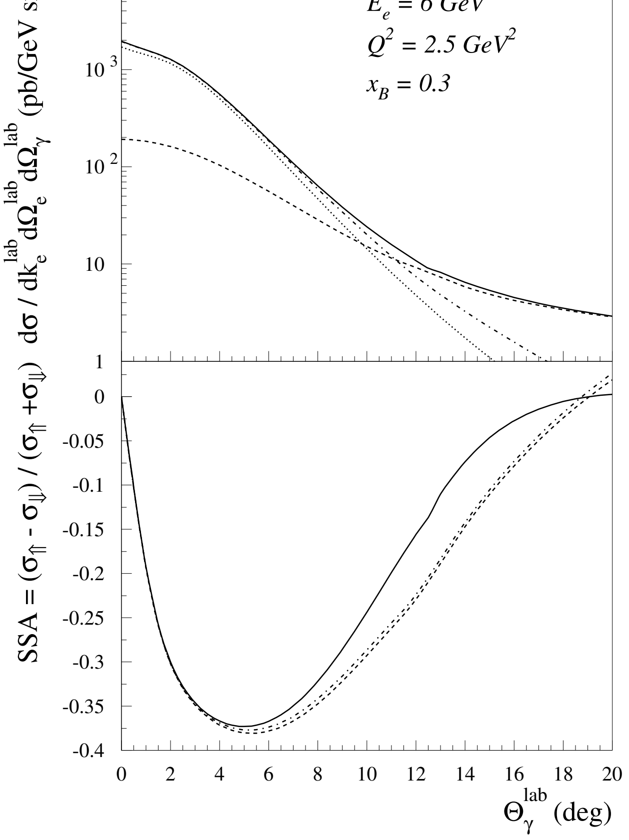

FIG. 15. Cross section (upper figure) and single-spin beam asymmetry (lower figure) in DVCS.

VII. HARD MESON ELECTROPRODUCTION

The generalized parton distributions can also be measured in hard meson electroproduction processes. The leading-twist pQCD contribution in this case involves a one-gluon exchange, which means that the hard subprocess is suppressed by the $\alpha_s/\pi \sim 1/10$ factor.

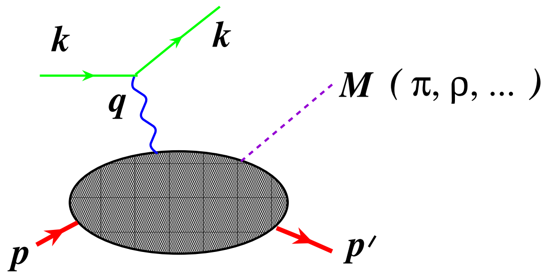

FIG. 16. Hard meson electroproduction process.

Calculating perturbatively the one-gluon-exchange amplitude, one gets the hard contribution in the form of a product of two nonperturbative functions: the distribution amplitude $\phi(\tau)$ of the relevant meson [integrated with $1/\tau$] and a generalized parton distribution $H(x,\xi;t)$ (or $E, \tilde{H}, \tilde{E}$) integrated with $1/(x-\xi+i0)$ or $1/(x+\xi-i0)$, the same integrals as in DVCS. In distinction to DVCS amplitude, which contains 4 GPD's $H(x,\xi;t)$, $E(x,\xi;t)$, $\tilde{H}(x,\xi;t)$ and $\tilde{E}(x,\xi;t)$, the nature of the produced meson "filters" the participating GPD's: vector meson production is sensitive to $H(x,\xi;t)$ and $E(x,\xi;t)$, while the amplitude of the hard pion electroproduction is expressed in terms of $\tilde{H}(x,\xi;t)$ and $\tilde{E}(x,\xi;t)$ only.

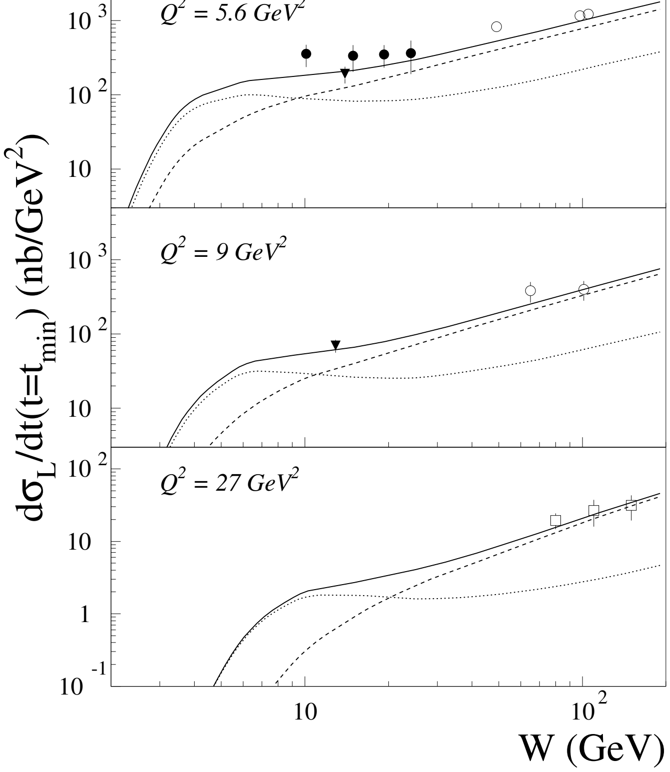

FIG. 17. Cross section for hard electroproduction of ρ meson by longitudinal photons.

Note that $\tilde{H}(x,\xi;t)$ reduces to $\Delta f(x)$ in the forward limit. In this sense, one can measure polarized parton distributions in this process without polarizing any participating particle.

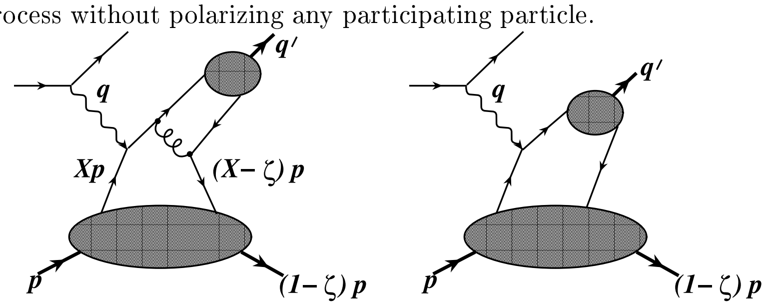

FIG. 18. QCD factorization for hard meson electroproduction. Left: asymptotically dominant hard gluon exchange contribution. Right: soft contribution.

One can also expect that for small t, the hadron spin-flip function $\tilde{E}(x,\xi;t)$ is dominated by the pion pole term $1/(t-m_\pi^2)$ and is proportional to the pion distribution amplitude $\varphi(X) \approx 6f_\pi X(1-X)$ taken at $X = x/\xi$. The relevant contribution is proportional to the pion EM form factor. The relative importance of $\tilde{H}(x,\xi;t)$ and $\tilde{E}(x,\xi;t)$ contributions varies with x_{Bj}: the pion pole terms dominate for x_{Bj} close to 1 while the $\tilde{H}$-terms are most pronounced for small x_{Bj} [29].

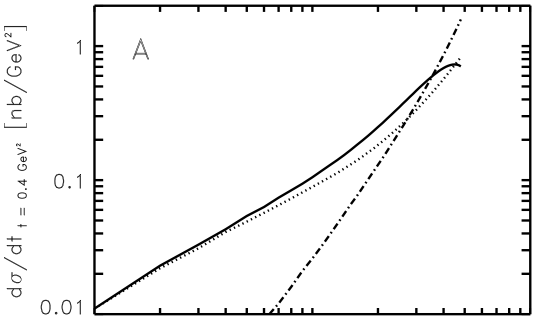

FIG. 19. Differential cross section for exclusive π^+ electroproduction through the scattering of longitudinally polarized photons from protons at $t = -0.4$ GeV^2 and $Q^2 = 10$ GeV^2 . The dotted and dot-dashed curves show the contributions due to $\tilde{H}$ and $\tilde{E}$ GPD's, respectively.

The flavor decomposition of the meson production amplitudes is also different from that of DVCS, thus giving a possibility to disentangle GPD's related to different quark flavors.

It is important to realize, however, that there is a competing soft mechanism [no hard gluon exchanges] which corresponds to a triple overlap of hadronic wave functions. It has a relative suppression M^2/Q^2 by a power of Q^2, with M^2 being a characteristic hadronic scale. If $M^2 \sim 1$ GeV^2, to clearly see the one-gluon-exchange signal one may need Q^2 above 10 GeV^2. A recent calculation [27] of the soft contribution gives a smaller value $M^2 \sim 0.5$ GeV^2 shifting the estimated onset of hard dominance to $Q^2 \sim 5$ GeV^2.

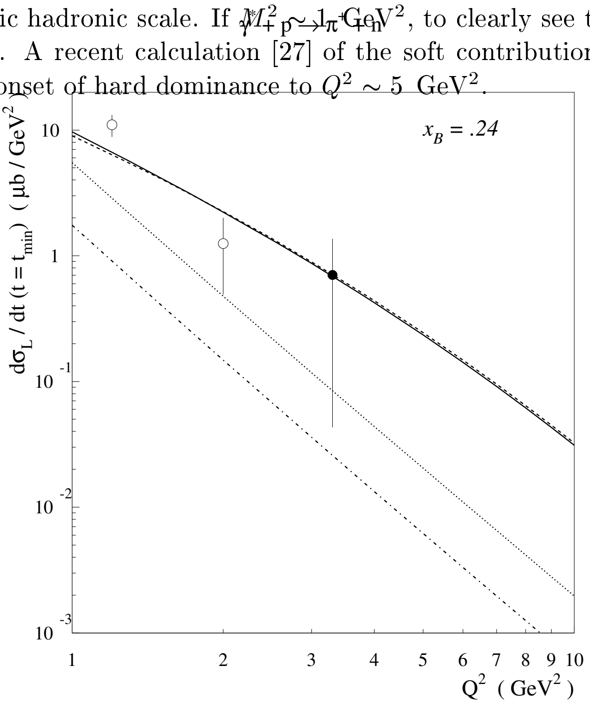

FIG. 20. Q^2-dependence of the differential cross section for exclusive π^+ electroproduction through the scattering of longitudinally polarized photons from protons at $t = t_{min}$ and $x_{Bj} = 0.24$. The dotted and dot-dashed curves show the contributions due to $\tilde{H}$ and $\tilde{E}$ GPD's, respectively.

VIII. WIDE-ANGLE REAL COMPTON SCATTERING.

Another Compton process in which the handbag contribution plays an essential role is wide-angle real Compton scattering. At moderately large $s, |t|, |u| \lesssim 10\ \mathrm{GeV}^2$, the leading-order contribution to WACS amplitude is given by the s- and u-channel handbag diagrams with hard quark propagators $(x\hat{P}+\hat{Q})/xs$ and $(x\hat{P}-\hat{Q})/xs$, respectively, where $P=(p+p')/2, Q=(q+q')/2$. Since skewedness in this case is equal to zero, one deals with the functions $\mathcal{F}^a(x,t) \equiv \mathcal{F}^a_{\zeta=0}(x;t) = H_a(x,\xi=0;t)$ and their $E, \tilde{H}, \tilde{E}$ analogs. The *nonforward parton densities* (ND's) $\mathcal{F}^a(x,t)$ are the simplest hybrids of parton densities and hadronic form factors. They are related to the usual parton densities by $\mathcal{F}^a(x,t=0)=f^a(x)$ and to form factors by

$$\sum_a e_a \int_0^1 \left[\mathcal{F}^a(x;t) - \mathcal{F}^{\bar{a}}(x;t)\right] dx = F_1(t) \, . \tag{8.1}$$

These relations are trivially satisfied by the factorized ansatz $\mathcal{F}^a_{val}(x;t) = f^a_{val}(x)F_1(t)$ [here $\mathcal{F}^a_{val}(x;t) \equiv \mathcal{F}^a(x;t) - \mathcal{F}^{\bar{a}}(x;t)$]. However, explicit calculations within the light-cone formalism suggest a more complicated interplay between the x- and t-behavior of ND's. In particular, assuming a relativistic Gaussian dependence $\exp[-k_\perp^2/2x\bar{x}\lambda^2]$ $(\bar{x} \equiv 1-x)$ of the hadronic wave function on the transverse momentum $k_\perp$, gives the model [24]

$$\mathcal{F}^a(x,t) = f^a(x) e^{\bar{x}t/4x\lambda^2} = \frac{f_a(x)}{\pi x \bar{x} \lambda^2} \int e^{-(k_\perp^2 + (k_\perp + \bar{x} r_\perp)^2)/2x\bar{x}\lambda^2} d^2 k_\perp \, . \tag{8.2}$$

The functions $f_a(x)$ here are the usual parton densities assumed to be taken from existing parametrizations like GRV, MRS, CTEQ, etc.

The basic scale λ specifies the average transverse momentum carried by the quarks. The magnitude of λ can be fixed from the relation (8.1) between $\mathcal{F}^a(x,t)$'s and $F_1(t)$ form factor. The best agreement with experimental data [34] in the moderately large t region $1\ \mathrm{GeV}^2 < |t| < 10\ \mathrm{GeV}^2$ is reached for $\lambda^2 = 0.7\ \mathrm{GeV}^2$ (see Fig.21). This value also gives a reasonable magnitude $\langle k_\perp^2 \rangle^u = (290\,\mathrm{MeV})^2$, $\langle k_\perp^2 \rangle^d = (250\,\mathrm{MeV})^2$ for the average transverse momentum of the valence u and d quarks in the proton. Similar models can be constructed for $F_2(t)$ and pion form factor $F_\pi(t)$ [36].

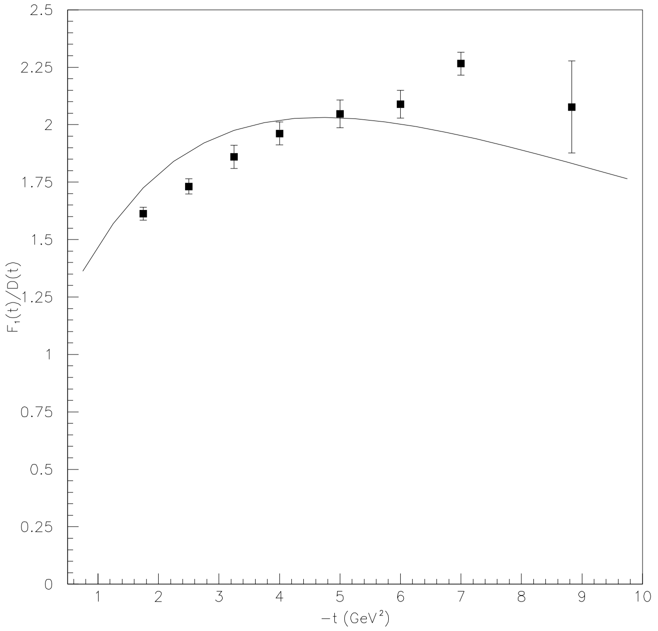

FIG. 21. Ratio $F_1^p(t)/D(t)$ of the $F_1^p(t)$ form factor to the dipole fit $D(t) = 1/(1-t/0.71\,\mathrm{GeV}^2)^2$. Curve is based on the model having a Gaussian $k_\perp$-dependence with $\lambda^2 = 0.7\,\mathrm{GeV}^2$.

It should be emphasized that the large-t real Compton scattering amplitude contains integrals

$$\int_0^1 \mathcal{F}(x;t)\,\frac{dx}{x}$$

with an extra $1/x$ factor. This results in a rather large enhancement of the Compton amplitude in the wide-angle regime. Keeping only the enhanced terms gives the WACS cross section as a product

$$\frac{d\sigma}{dt} \approx \frac{2\pi\alpha^2}{\tilde{s}^2}\left[\frac{(pq)}{(pq')}+\frac{(pq')}{(pq)}\right] R_1^2(t)\,, \tag{8.3}$$

of the Klein-Nishina cross section and the square of a new effective form factor $R_1(t)$. In the model of ref. [24], $R_1(t)$ is given by

$$R_1(t) = \sum_a e_a^2 \int_0^1 f_a(x) e^{\bar{x}t/4x\lambda^2}\,\frac{dx}{x}\,. \tag{8.4}$$

Comparison with existing data [30] is shown in Fig.22. The curves from [24] follow the data pattern but are systematically lower by a factor of 2, which may be explained by the fact that several terms were neglected, each capable of producing up to a 20% correction in the amplitude. Thus the agreement between the curves and the data may be considered as encouraging.

The angular dependence for the combination $s^6(d\sigma/dt)$ is shown on Fig.22a. All the curves for initial photon ehergies 2,3,4,5 and 6 GeV intersect each other at $\theta_{\rm cm} \sim 60°$. This is in good agreement with experimental data of ref. [30] where the differential cross section at fixed cm angles was fitted also by powers of s: $d\sigma/dt \sim s^{-n(\theta)}$ with $n^{\rm exp}(60°) = 5.9 \pm 0.3$. The curves of Ref. [24] correspond to $n^{\rm soft}(60°) \approx 6.1$ and $n^{\rm soft}(90°) \approx 6.7$ which also agrees with the experimental result $n^{\rm exp}(90°) = 7.1 \pm 0.4$.

This can be compared with the scaling behavior of the asymptotic hard contribution: modulo logarithms contained in the α_s factors, they have a universal angle-independent power $n^{\rm hard}(\theta) = 6$. For this reason, it is very important to perform precision measurements of $n(\theta)$ in future experiments at Jefferson Lab [35].

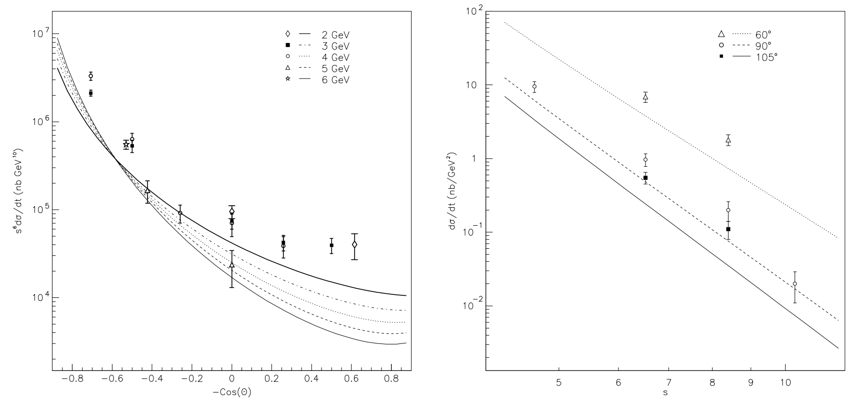

FIG. 22. a) Angular dependence of the combination $s^6(d\sigma/dt)$. b) s-dependence of the differential cross section $d\sigma/dt$ for $\theta = 60°$ (dotted line), $\theta = 90°$ (dashed line) and $\theta = 105°$ (solid line).

Above picture for the large-s, high-t behavior of the real Compton amplitude implies that the large-t behavior of the form factor type matrix elements is determined by an overlap of soft components of hadronic wave functions. It should be mentioned that for extremely large $|t| \gg 10\,\mathrm{GeV}^2$ this mechanism is subdominant. The dominant contribution is provided by purely hard contributions involving two-gluon exchange diagrams. The hard contribution was recently recalculated by Brooks and Dixon [33].

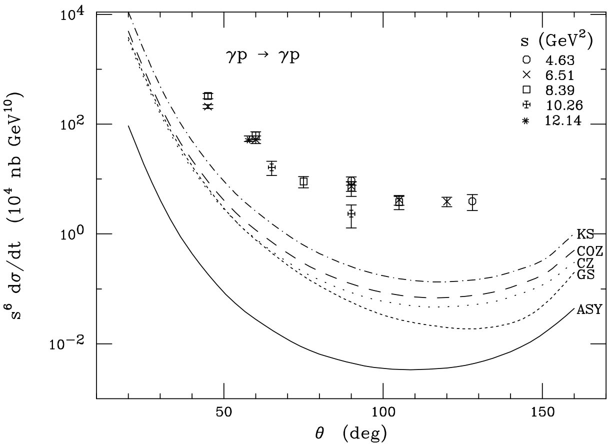

FIG. 23. Hard contribution to the wide-angle Compton scattering cross section calculated for "humpy" (KS,COZ,CZ and GS) and asymptotic (ASY) nucleon distribution amplitudes [33].

Their result for the hard contribution is below the data by an order of magnitude for "humpy" distribution amplitudes and by two orders of magnitude for the asymptotic shape of the nucleon DA. This gives another evidence that the handbag contribution is important at JLab energies. The spin structure of the hard contribution is also different from that predicted by the handbag mechanism.

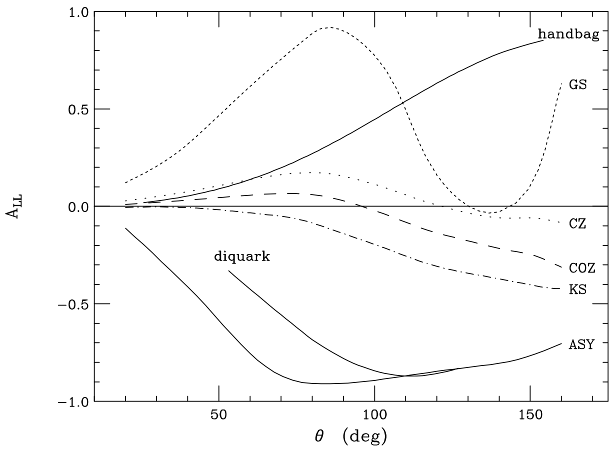

FIG. 24. The initial state helicity correlation A_{LL} for hard perturbative QCD contribution (with GS,CZ,COZ,KS and ASY distribution amplitudes), for diquark model and for handbag model [33].

Thus, the experiment with a polarized photon beam is capable to demonstrate what is the dominant reaction mechanism at JLab energies.

IX. CONCLUSIONS

The study of hard exclusive electroproduction processes opens a new area for exploration of hadronic structure. Generalized parton distributions provide a unified description of different exclusive and inclusive reactions. Deeply virtual Compton scattering is a remarkable example of Bjorken scaling phenomena in exclusive processes and the cleanest supplier of information about GPD's. Hard meson electroproduction can provide complementary information about GPD's and is the best candidate to unravel the pQCD hard gluon exchange in exclusive reactions.

---

[1] R. P. Feynman, *The Photon-Hadron Interaction* (Benjamin, Reading 1972).

[2] V. L. Chernyak and A. R. Zhitnitsky, JETP Letters, **25**, 510 (1977);
V. L. Chernyak, A. R. Zhitnitsky and V. G. Serbo, JETP Letters **26**, 594 (1977).

[3] D. R. Jackson, Thesis, CALTECH, 1977 (unpublished);
G. R. Farrar and D. R. Jackson, Phys. Rev. Lett. **43**, 246 (1979).

[4] A. V. Radyushkin, JINR report P2-10717, Dubna, 1977 (unpublished).

[5] A. V. Efremov and A. V. Radyushkin, JINR preprint E2-11983, Dubna (October 1978), published in Theor. Math. Phys. **42**, 97 (1980).

[6] S. J. Brodsky and G. P. Lepage, Phys. Lett. **87B**, 359 (1979).

[7] S. J. Brodsky and G. P. Lepage, Phys. Rev. **D22**, 2157 (1980).

[8] X. Ji, Phys. Rev. Lett. **78**, 610 (1997); Phys.Rev. D **55** (1997) 7114.

[9] A.V. Radyushkin, Phys. Rev. D **56**, 5524 (1997).

[10] J.C. Collins, L. Frankfurt and M. Strikman, Phys. Rev. D **56** (1997) 2982.

[11] D. Müller, D. Robaschik, B. Geyer, F. -M. Dittes and J. Hořejši, Fortschr. Phys. **42**, 101 (1994).

[12] X. Ji and J. Osborne, Phys.Rev. D 58, 094018 (1998).

[13] J. C. Collins and A. Freund, Phys.Rev. D **59**, 074009 (1999).

[14] I. V. Musatov and A. V. Radyushkin, Phys. Rev. D **61** (2000) 074027.

[15] V.Yu. Petrov et al. Phys.Rev. D **57** (1998) 4325.

[16] A.V. Radyushkin, Phys. Rev. D **59** (1999) 014030.

[17] A.V. Radyushkin, Phys. Lett. B **449** (1999) 81.

[18] A.V. Radyushkin, Phys. Lett. B **131** (1983) 179.

[19] X. Ji, W. Melnitchouk and X. Song *Phys. Rev.* D **56**, 5511 (1997).

[20] V.Yu. Petrov et al. *Phys. Rev.* D **57**, 4325 (1998).

[21] M. Diehl, T. Feldmann, R. Jakob and P. Kroll, *Eur. Phys. J.* C **8**, 409 (1999).

[22] L. Mankiewicz, G. Piller and T. Weigl, *Eur. Phys. J.* C **5**, 119 (1998).

[23] A.V. Radyushkin, Phys. Lett. B **380**, 417 (1996)

[24] A.V. Radyushkin, Phys. Rev. D **58** (1998) 114008.

[25] X.Ji, J. Phys. G **24** (1998) 1181.

[26] CLEO Collaboration (J. Gronberg et al.), Phys.Rev. D **57** (1998) 33.

[27] M. Vanderhaeghen, P.A.M. Guichon and M. Guidal, *Phys. Rev.* D **60**, :094017 (1999).

[28] M. Vanderhaeghen, P.A.M. Guichon and M. Guidal, Phys.Rev.Lett. **80** (1998) 5064, Phys.Rev. D **60**, 094017 (1999); P.A.M. Guichon and M. Vanderhaeghen, Prog.Part.Nucl.Phys. **41**, 125-190 (1998).

[29] L. Mankiewicz, G. Piller and A. Radyushkin, *Eur. Phys. J.* C **10**, 307 (1999).

[30] M.A. Shupe et al. Phys.Rev. D **19**, 1921 (1979).

[31] I.V. Anikin, B. Pire and O.V. Teryaev, hep-ph/0003203.

[32] A. M. Nathan, E97-108 collaboration, hep-ph/9807397.

[33] T. Brooks and L. Dixon, hep-ph/0004143.

[34] L. Andivahis et al. Phys. Rev. D **50** (1994) 5491.

[35] A. M. Nathan, E97-108 collaboration, hep-ph/9807397.

[36] A. V. Afanasev, hep-ph/9910565.